HHS Public Access

Author manuscript

Cell Physiol Biochem. Author manuscript; available in PMC 2020 August 28.

Published in final edited form as:

Cell Physiol Biochem. 2019 ; 52(3): 503–516. doi:10.33594/000000036.

Establishing a Link between Endothelial Cell Metabolism and Vascular Behaviour in a Type 1 Diabetes Mouse Model

Carolina Silva[a,b], **Vasco Sampaio-Pinto**[b,c,d], **Sara Andrade**[a,b,e], **Ilda Rodrigues**[a], **Raquel Costa**[a,b], **Susana Guerreiro**[a,b,f], **Eugenia Carvalho**[g,h,i], **Perpétua Pinto-do-Ó**[b,c,d], **Diana S. Nascimento**[b,c,d], **Raquel Soares**[a,b]

[a]Department of Biomedicine, Unit of Biochemistry, Faculty of Medicine of the University of Porto, Porto, Portugal

[b]i3S, Instituto de Investigação e Inovação em Saúde, Universidade do Porto, Porto, Portugal

[c]Instituto Nacional de Engenharia Biomédica, Universidade de Porto, Porto, Portugal

[d]Instituto de Ciências Biomédicas Abel Salazar, Universidade do Porto, Porto, Portugal

[e]Instituto de Patologia e Imunologia Molecular da Universidade do Porto, Porto, Portugal

[f]Faculdade de Ciências da Nutrição e Alimentação, Universidade do Porto, Porto, Portugal

[g]Center of Neuroscience and Cell Biology, University of Coimbra, Coimbra, Portugal

[h]The Portuguese Diabetes Association, Lisbon, Portugal

[i]Department of Geriatrics, University of Arkansas for Medical Sciences, Little Rock, United States

Abstract

Background/Aims: Vascular complications contribute significantly to the extensive morbidity and mortality rates observed in people with diabetes. Despite well known that the diabetic kidney and heart exhibit imbalanced angiogenesis, the mechanisms implicated in this angiogenic paradox remain unknown. In this study, we examined the angiogenic and metabolic gene expression profile (GEP) of endothelial cells (ECs) isolated from a mouse model with type1 diabetes *mellitus* (T1DM).

Methods: ECs were isolated from kidneys and hearts of healthy and streptozocin (STZ)-treated mice. RNA was then extracted for molecular studies. GEP of 84 angiogenic and 84 AMP-activated Protein Kinase (AMPK)-dependent genes were examined by microarrays. Real time PCR

Raquel Soares, Department of Biomedicine, Faculty of Medicine, University of Porto, Al Prof Hernâni Monteiro 4200-319 Porto (Portugal), Tel. +351225513624, raqsoa@med.up.pt.

AUTHOR CONTRIBUTION: CS and RS participated in the design and conception of the study; CS performed the whole laboratory and statistical analyses and drafted the manuscript; VSP, PPO, DSN carried out the FACS assay design and data acquisition, as well as the interpretation of FACS data; SA advised and performed microarray and RT-PCR assays; IR headed the parafin embedded tissue and histologial staining; SG, EC were responsible for the animal studies and immunohistochemistry analyses; RC advised the methodological laboratorial analysis and animal studies; RS and EC critically revised the manuscript for important intellectual content. All authors were involved in drafting and revising the article. All authors read and approved the final version of the manuscript.

Disclosure Statement

No conflict of interest.

confirmed the changes observed in significantly altered genes. Microvessel density (MVD) was analysed by immunohistochemistry, fibrosis was assessed by the Sirius red histological staining and connective tissue growth factor (CTGF) was quantified by ELISA.

Results: The relative percentage of ECs and MVD were increased in the kidneys of T1DM animals whereas the opposite trend was observed in the hearts of diabetic mice. Accordingly, the majority of AMPK-associated genes were upregulated in kidneys and downregulated in hearts of these animals. Angiogenic GEP revealed significant differences in *Tgfβ*, Notch signaling and *Timp2* in both diabetic organs. These findings were in agreement with the angiogenesis histological assays. Fibrosis was augmented in both organs in diabetic as compared to healthy animals.

Conclusion: Altogether, our findings indicate, for the first time, that T1DM heart and kidney ECs present opposite metabolic cues, which are accompanied by distinct angiogenic patterns. These findings enable the development of innovative organ-specific therapeutic strategies targeting diabetic-associated vascular disorders.

Keywords

Carbohydrate and lipid metabolism; Cell sorting; Endothelium metabolism; Genomics; Micro and macrovascular complications

Introduction

Type 1 diabetes *mellitus* (T1DM), is an autoimmune disorder characterized by beta cell failure, consequently resulting in decreased insulin release. Generally, *β*-cell failure is mediated by immune mechanisms, but its etiopathogenesis is not fully understood.

Glycemic variability is nowadays considered a key factor for the development of T1DM complications. Moreover, the chronic hyperglycemic state characteristic of DM, among other processes, can lead to macro and microvascular complications, namely diabetic retinopathy, nephropathy and peripheral neuropathy. These processes can evolve, resulting in blindness, renal failure, and foot ulcer development respectively.

In addition to the extensively morbid conditions, including limb amputations, neuropathic problems like Charcot joints and autonomic neuropathy, prolonged diabetes can also cause gastrointestinal, genitourinary problems, as well as sexual dysfunction [1]. Moreover, T1DM patients have a 10-fold increased risk of developing cardiovascular disease when compared to normoglycemic subjects [2, 3], with coronary artery disease being the main cause of morbimortality in these patients [4].

Angiogenesis, the process by which new blood vessels are formed from pre-existing ones, when persistent and uncontrolled, is the main characteristic for vascular abnormalities and it is often impaired in diabetic patients [5]. A key regulator of angiogenesis is the tight equilibrium between angiogenic inhibitors and stimulators [6]. An important feature of T1DM is the existence of the so-called “angiogenic paradox”, a phenomenon in which the patient simultaneously presents accelerated angiogenesis in certain organs, such as the eye (retinopathy), kidney (nephropathy), in addition to atherosclerotic plaque progression, and

decreased angiogenesis in others, preventing wound healing and impairing artery collateral formation [7, 8].

Vascular metabolism is altered not only in T1DM, but also in other types of diabetes (type 2 DM and gestational DM).

AMPK is an energy sensor that targets carbohydrate and lipid metabolism by phosphorylating enzymes and modulating gene expression [9]. AMPK is an insulin sensitizing molecule, rendering it an ideal therapeutic target. As a result, several pharmacological agents, including metformin and thiazolidinediones, activate AMPK signaling pathways, one of the reasons they are currently used for diabetes treatment. Interestingly, in endothelial cells (ECs), AMPK activation by these vasculoprotective agents triggers several benefic physiological effects in diabetic vascular complications [10, 11]. Therefore, given the high morbidity and mortality rates associated with micro and macrovascular complications in diabetic patients, it is of paramount importance to highlight the AMPK-associated metabolic changes present in ECs of the distinct organs and their association with angiogenic imbalance.

The aim of the current study was to analyse the expression pattern of genes associated with metabolism and angiogenesis in kidney and heart ECs from T1DM mice. To address this, we isolated ECs by flourescence-activated cell sorting (FACS) and performed gene microarray assays to assess the AMPK-dependent and angiogenic gene expression profile in these specific organs.

Materials and Methods

Type 1 Diabetes animal model

Twenty-five twelve-week-old male C57Bl/6 mice (Charles River, Saint-Germain-Nuelles, France) were used in this study. Mice were kept under controlled conditions of humidity (35 ± 5%) and temperature (23 ± 5 °C), on a 12-hour light/dark cycle and had access to water and rodent chow *ad libitum*. Animals were randomly assigned into two experimental groups: 12 control (CTR) and 13 STZ-treated mice. As recommended by the NIH Animal Models of Diabetes Complication Consortium (Low dose protocol), T1DM was induced by intraperitoneal administration of STZ (Sigma-Aldrich, Portugal), for five consecutive days, at a dose of 50mg/kg body weight dissolved in 0.1M citrate buffer (pH 4.5). Fourteen days after the last STZ injection, mice were considered diabetic when they presented blood glucose levels above 250mg/dL. No adverse events were observed in the experimental group. Control animals were administered with the same volume of saline solution. Body weight and glycemia were monitored three times per week. After 10 weeks following diabetes onset, all animals were euthanized and organs were removed. Kidneys and hearts of 4 CTR and 6 STZ-treated animals were used for isolation of ECs by FACS. The kidneys and the left ventricle of the remaining animals were fixed in formalin and paraffin-embedded for histological analyses. All animal studies were performed by certified technicians. All animal care and procedures were in accordance with the Portuguese Act 1005/92 and European Community guidelines for the use of Experimental Animal studies. The guide for the care and use of laboratory animals, 8th edition (2011) was followed.

Fluorescence-activated cell sorting (FACS)

FACS was performed to isolate ECs from the heart and kidney. Both organs were digested using tissue-specific protocols of GentleMACS Dissociator in Hank's balanced salt solution (HBSS) (H9269, Sigma-Aldrich®, Portugal) containing collagenase II (CLS-2, Worthington, USA) at 6, 5 mg/ml concentration for heart and collagenase IV (CLS-4, Worthington, USA) at 1mg/ml concentration for kidney. Both solutions had DNase (A3778, VWR, Portugal) at 60U/ml.

The suspension was filtered and the cellular portion was collected. The cellular suspension was mixed with HBSS with 10% FBS to neutralize enzymatic activity and centrifuged at 300xg for 10 minutes. Erythrocyte depletion was accomplished by osmotic shock as deyonized water was added to the pellet and kept under stirring for 11 seconds. FACS medium (0.01% sodium azide and 3% FBS in PBS) was immediately added to interrupt osmolysis and cells were centrifuged again. Cells were evenly distributed for each staining in a round bottom multi-well plate and incubated during 30 min with the respective antibody mix: CD31-PeCy7 (Rat IgG2a; eBiosciences - 25–0311), CD31-APC (Rat IgG2a; Biolegend – 102516); CD45-PeCy7 (Rat igG2b, k; eBiosciences - 25–0451), CD45-PE (Rat IgG2b, k; eBioscience - 12–0451-82); CD54-APC (Rat IgG2b, κ; Biolegend – 116120), CD90-FITC (Rat IgG2b, k; Biolegend – 105305);, TER119-PeCy7 (Rat IgG2b, k; Biolegend – 116221), TER119-PE (Rat IgG2b, k; Biolegend – 116208); CD105-PE (Rat IgG2a, k; Biolegend – 120407 and CD106-PE (Rat IgG2a, k; Biolegend - 105713) at 1:100 dilution, on ice and in the dark. Cells were washed twice in FACS media and transferred to FACS tubes.

In order to exclude nonviable cells from the analysis, 0.5% of propidium iodide (PI) (P4170, Sigma-Aldrich) was added to the cell suspension 1–2 min prior to analysis. Fifty thousand events (of appropriate size and complexity) per staining were acquired in the cytometer FACS ARIA (BD Biosciences). Subsequent analysis and graphing were performed in the FlowJo VX software.

RT^2 PROFILER PCR arrays

Total RNA was extracted from isolated ECs of the kidney and heart by Quiagen RNeasy Micro kit (Werfen, Castellbisbal, Spain). After extraction and in accordance with the manufacturer, an identical amount of RNA for each sample (27 ng) was converted into cDNA and pre-amplified using primers specifically designed for the subsequent arrays by RT^2 PreAMP Pathway Primer Mix (Werfen, Taracon-Cuenca, Spain). Three samples from each group were selected for analysis by Angiogenesis and AMPK RT^2 Profiler PCR Arrays (Werfen, Castellbisbal, Spain). Each array evaluated the expression of 84 key genes involved in the angiogenic process or in the AMPK signaling pathway, as well as 5 housekeeping genes. Plates were prepared and ran on Light Cycler 96 thermal cycler (Roche, Mannheim, Germany), following manufacturer's instructions. Relative gene expression was determined using the $\Delta\Delta C_T$ method and data was analyzed using the PCR Array Data Analysis Web Portal (Quiagen). Differentially-expressed genes relative to healhy controls were defined by the p-values obtained in the microarray's analysis software.

Quantitative Real Time-PCR (qRT-PCR)

The remaining total RNA was used to validate the arrays results. cDNA was synthesized using PrimeScript™ RT reagent Kit and was pre-amplified according to the protocol provided in SsoAdvanced™ PreAmp Supermix (Bio-Rad, Hercules, CA). Primers for mouse *Adra1a*, *Adra2c*, *Cpt1a*, *Jag1*, *Pfkfb2*, *Pnpla2*, *Smad5*, *Tgfb2* and *Timp2* were used and *Gapdh* as the housekeeping gene (sequences provided in Table 1). This reaction was performed in the LightCycler® 96 System (Roche, Mannheim, Germany) and each cDNA sample was used in duplicate as template for qRT-PCR. Relative gene expression was analyzed using the Livak method ($2^{-\Delta\Delta C_T}$).

Immunohistochemistry assay for CD31

Paraffin-embedded kidney and left ventricle tissue were cut into 3-μm sections. The Rat Detection Kit for Anti-Mouse CD31 (Biocare Medical, Pacheco, CA, USA) was used according to the supplied protocol in order to evaluate the microvascular density. The antibody against CD31 (Biocare Medical, Pacheco, CA, USA) was diluted 1:50 in Da Vinci Green diluent, provided in the kit.

Vessels were counted in approximately twenty non-overlapping fields (200x magnification) of each organ and normalized to the total tissue area. Any positively-stained endothelial cell or cluster of cells that was separated from adjacent vessels was considered as an individual vessel.

Fibrosis analysis

Sirius Red histological staining.—Fibrosis was evaluated in kidney and left ventricle tissues by Sirius Red histological staining in parafin-embedded sections. Ten representative images (100x magnification) of each animal were obtained and fibrosis was calculated as the percentage of the red stained area and normalized to the total tissue area by the FIJI Software [12].

Connective tissue growth factor (CTGF) quantification by ELISA.—Quantification of CTGF was performed in heart and kidney homogenates of diabetic and control animals using a commercial Mouse CTGF ELISA kit (LSBio-LifeSpan BioSciences, WA, USA), according to the manufacturer instructions. Absorbance was read at 450mm and the results analysed in GraphPad Prism 6.0 Software (GraphPad Software Inc., CA, USA).

Statistical analysis

All results were expressed as the mean ± SEM and were analysed in the GraphPad Prism 6.0 Software (GraphPad Software Inc., CA, USA), with a confidence interval of 95% and p value < 0,05 by t test.

Results

Body weight and glycemia monitoring

When compared to controls, STZ-treated mice presented a sustained decrease in body weight during the whole experiment, although without reaching statistical significance (Fig.

1A). As expected, diabetic mice exhibited significantly increased blood glucose levels throughout the 10-week experimental period (Fig. 1B). Both findings confirmed the diabetic status of STZ-treated mice.

ECs quantification and microvessel density in kidney and heart

Heart and kidney from diabetic and control animals were homogeneized and analysed by flow cytometry. ECs were identified by the expression of CD31, following exclusion of hematopoietic cells ($CD45^+$) and erythrocytes ($TER\text{-}119^+$). Interestingly, when compared to controls, the kidney of STZ-treated mice were significantly enriched in ECs (3.857±0.5845 vs. 2.078±0.3644; p=0.053) (STZvsCTR), whereas in the heart an opposite trend was observed (Fig. 2A and 2B).

To further confirm these findings, MVD was assessed by immunohistochemistry analysis in paraffin-embedded sections. MVD, obtained by the ratio between the number of vessels and the total tissue area (mm^2), showed an opposite angiogenic profile in both organs of STZ-treated mice, when compared to healthy animals. While the number of blood vessels was increased in the kidney cortex of STZ-treated animals relative to the controls, a decrease in MVD was observed in the hearts of this group, (Fig. 2C).

Angiogenic gene expression profile in kidney and heart ECs

We next performed PCR microarrays for angiogenic markers in FACS-sorted ECs from both organs (Table 2 and 3). From the 84 genes examined, 10 were upregulated and 74 were downregulated in ECs from the STZ-treated heart, compared to controls (Table 2). Among these, the *Notch1*-ligand *Jagged1* gene was significantly downregulated whereas *Smad5*, and the *Transforming growth factor* (*Tgf*) β signaling effector protein were significantly upregulated (Table 2). In ECs from T1DM kidney, 36 genes were upregulated, whereas 48 were downregulated in comparison to controls (Table 3). However, only the *Tgf*β2, *Kinase insert domain receptor (Kdr*) and the tissue inhibitor of metalloproteinases (*Timp*) 2 were significantly downregulated in renal ECs from STZ-treated animals relatively to healthy controls (Table 3).

Interestingly, most of the genes encoding for antiangiogenic factors were upregulated in heart and downregulated in the kidney (Fig. 3). These findings are in agreement with the angiogenesis imbalance previously observed in the heart and kidney, respectively.

Fibrosis evaluation in hearts and kidneys

Our angiogenic microarray assays revealed that the TGFβ signalling pathway was altered in both heart and kidney of T1DM animals. The fact that TGFβ is involved in fibrosis prompted us to examine whether this process was affected in the hearts and kidneys of diabetic animals. Fibrosis was analysed by Sirius Red histological staining in tissue sections of both organs collected from STZ-treated and control animals. Interestingly, diabetic animals showed a tendency for an increase in the fibrotic area in both heart and kidney, although not reaching statistical significance (Fig. 4A). Quantification of Connective tissue growth factor (CTGF), an important marker for fibrosis, exhibited the same trend in both diabetic organs (Fig. 4B).

AMPK-dependent gene expression profile in heart and kidney of T1D mice

Knowing that cellular behavior depends on energy metabolism, we next investigated the expression pattern of 84 genes associated with the AMP-depending kinase, an energy-sensing enzyme. Remarkably, kidneys and hearts presented opposite expression profiles as illustrated in Fig. 5. The AMPK-associated gene expression pattern was mostly upregulated in kidney ECs from diabetic animals in comparison to controls, while in hearts it was primarily dowregulated (Table 4 and 5). Significantly upregulated genes in diabetic kidney ECs are involved in carbohydrate *(Pfkfb2, Gusb)* and lipid *(Cpt1a)* catabolic pathways and adrenoceptor signaling (Adra1a), as well as cell growth, migration and autophagy *(Rb1cc1*), and AMPK signaling *(Strada, Prkaa1*). On the other hand, significantly downregulated genes in ECs from diabetic hearts are implicated in signaling pathway cascades (*Cab39*, *Akt2*, *Rps6kb2*, *Adra2c, Prkacb*), as well as in triglyceride hydrolysis (*Pnpla2*). Genes that were significantly different in the microarrays were validated also by qRT-PCR.

Discussion

The concept of the angiogenic paradox was first described by Waltenberg et al. [13] who reported that chronic diabetes *mellitus* is associated with both impaired (collateral growth and wound healing) or enhanced (retinopathy and nephropathy) angiogenesis [14]. Substantiating findings were then reported by others in the literature. Using a type 2 diabetes animal model, our group has also observed increased number of microvessels in kidneys and decreased in left ventricle of diabetic mice when compared to controls [15]. By isolating ECs from mouse hearts and kidneys, the current study provides molecular evidence for this angiogenic paradox in a T1DM animal model. We were able to concurrently address the expression pattern of genes related with angiogenesis and cell energy metabolism.

Diabetic conditions of the STZ-treated mice were first established by the observed sustained reduced weight and hyperglycemia during the experimental protocol. We then found that mice presented increased number of blood vessels in kidneys and reduced in hearts, as confirmed by FACS and microvessel density assessed by immunohistochemistry. T1DM heart ECs exhibited a significant upregulation of BMP/TGFβ signaling effector *Smad5*. BMP and TGFβ bind type II receptor (TβRII), which in turn activates type 1 receptor (TβRI). In ECs, there are two TβRI (activin receptor-like kinase (ALK)1 and ALK5), resulting in activation of two distinct SMADs signaling pathways. By binding to ALK1, TGFβ phosphorylates SMAD1, 5 and 8, resulting in transcription of genes implicated in cell proliferation, diferentiation and migration. Conversely, TGFβ signaling through ALK5 results in SMAD2 and 3 recruitment, inhibiting these genes [16]. Interestingly, when ALK1 is activated by BMP9, EC proliferation, migration and sprouting is inhibited [17, 18]. Therefore, ECs will behave differently depending on the ligand, as well as on the ALK receptor being activated. According to our results, *Tgfβ* did not significantly change in diabetic heart when compared to healthy animals, implying that *Smad5* upregulation in heart ECs might promote ALK1 activation through BMP, which ends in angiogenesis inhibition.

Concomitantly, diabetic hearts also presented reduction in the Notch ligand *Jagged1*. The Notch signaling pathway consists of a highly conserved family of four membrane receptors (Notch1–4) and two transmembrane ligands: Jagged (1–2) and Delta-like (Dll) (1, 3 and 4)

which are involved in cell growth, differentiation and tissue remodelling [19]. By binding to its ligands in a neighboring cell surface, the intracellular Notch domain (NICD) translocates to the nucleus, ultimately leading to target gene activation [20, 21]. In blood vessels, Notch has been implicated in angiogenesis [22, 23]. But in contrast to DLL4, Jagged1 expression in ECs has proangiogenic functions, thus antagonizing DLL4/Notch signaling and inducing vascular maturation and tumor growth [23–25]. Therefore, our findings that *Jagged1* is actually downregulated in diabetic hearts is in agreement with the reduced number of microvessels observed. Remarkably, *Jagged1* was reported to be a TGFβ target gene, through ALK5-induced SMAD3 [26]. Taking into account that SMAD3 and SMAD5 are activated by opposite receptors, *the* overexpression of *Smad5* observed in diabetic heart may explain the *Jagged1* downregulation, and consequently the observed reduction in angiogenesis. These findings were corroborated by the metabolic gene expression profile found in T1DM hearts. Accordingly, Akt, Erk and p38 MAPK are downstream effectors of several membrane receptors involved in processes such as cell division and migration. These cytoplasmic kinases were downregulated in heart ECs, implying impairment of angiogenesis.

Conversely, diabetic kidneys presented exacerbated angiogenesis as found by the increased number of ECs (FACS analysis), as well as mcirovessel density. This behavior was documented by the downregulation of *Timp2*, an inhibitor of matrix metalloproteinases, *Kdr* and *Tgfβ2*. Besides participating in matrix remodeling and angiogenic process, TIMP2 is also associated with inflammation and tumor growth [27]. The reduced expression of *Timp2* enables extracellular matrix (ECM) degradation, explaining the proangiogenic phenotype observed in this organ in diabetic mice. Moreover, TIMP expression accompanies TGFβ. According to Ruiz-Ortega et al. [28] TGFβ stimulates TIMP expression. TGFβ plays activating and inhibiting multifunctional roles in a wide variety of cells [28–30]. Interestingly, low concentrations of TGFβ induce cell growth, whereas, at higher concentrations, this growth factor is able to prevent proliferation of smooth muscle cells [31]. In agreement, the observed TGFβ downregulation may result in EC proliferation, and consequently in a proangiogenic phenotype. According to these findings, the TGFβ pathway is a putative therapeutic target to address diabetic vascular complications. We also found that *Kdr* mRNA was downregulated in T1DM kidneys. KDR is activated by VEGF binding, resulting in vessel sprouting. Nevertheless, *Kdr* downregulation was obtained in ECs isolated from the whole diabetic kidney and not from the kidney cortex where increased angiogenesis is well established in diabetes [32]. In addition, our findings were obtained in animals already presenting diabetes for 10 weeks, where sprouting had already occurred and resulted in mature stabilized vessels, which no longer expressed *Kdr*. Supporting our findings, Cooper et al. compared the expression of *Kdr* at 3 weeks and 32 weeks upon STZ treatment in a T1DM rat model, and observed that although *Kdr* was upregulated at 3 weeks, the receptor expression was diminished at the later stages [32].

Interestingly, renal ECs overexpressed AMPK-associated genes implicated in catabolism. PFK-2/FBPase-2 (6-phosphofructo-2-kinase/fructose-2, 6-bis-phosphatase) is a bi-functional homodimeric enzyme that presents both kinase and phosphatase activity [33]. PFKFB2, one of the four isoforms identified (1, 2, 3 and 4), is expressed in heart and kidney [33, 34]. In this study, *Pfkfb2* was significantly upregulated in kidney ECs of T1DM mice. The Pfkfb3

isoform expression was also upregulated in these cells (10-fold increase), although not in a significant manner (data not shown). Glucose is a primary energy source for ECs and recent studies revealed that PFKFB3 plays a critical role as a regulator of glycolysis. During vessel sprouting, PFKFB3 drives glycolysis in tip cells and inhibits the stalk cell behavior by Notch signaling [35–37]. Using a T2DM mouse model, our group recently showed that this enzyme was upregulated in kidney and downregulated in left ventricle [15] Concomitantly, the number of microvessels as well as the expression of the phosphorylated (active) form of VEGFR2 accompanied this PFKFB3 expression. Thus, the current findings in T1DM corroborated our previous study in a type 2 DM mouse model [15], reinforcing the association between glycolysis activity and angiogenesis.

Although glycolysis is the favourite metabolic pathway for energy supply, fatty acid oxidation has also been shown to play an important role in stalk cell metabolism and synthesis of deoxynucleotide triphosphates (dNTPs) [35]. The carnitine palmitoyl transferase 1A (CPT1A) enzyme favours the translocation of long chain fatty acids into the mitochondria where they can be oxidized. The observed upregulation of this gene in diabetic kidney enables fatty acids entry into the mitochondria, hence resulting in energy production and redox homeostasis, providing fuel for EC proliferation, migration and vessel assembly. In agreement, *Rb1cc1*, implicated in cell proliferation, migration and autophagy, was also upregulated.

A remarkable finding of the current study was the complete distinct metabolic gene profile found in ECs from diabetic kidneys and hearts. Whereas most AMPK-associated genes were overexpressed in kidney ECs, while in heart ECs the majority of AMPK pathway genes were downregulated (Fig. 5A and 5B). AMPK is activated in several types of cells by different stimuli, controling metabolic processes through phosphorylation of key essential markers [38]. In ECs, AMPK activity can be stimulated by changes in ATP levels, regulating fatty acid oxidation, glycolysis, nitrite oxide synthesis, inflammation and angiogenesis [38]. Overall, AMPK signaling pathways are reduced in DM, therefore a potential therapeutic target. AMPK activation induces insulin sensitivity and glucose utilization [39].

Another important feature of this study is the fact that despite the opposite molecular landscape observed in heart and kidney ECs, both organs presented increased fibrosis as evaluated by histological staining. Tissue fibrosis is a common feature in diabetes, associated with hyperglycemia, advanced glycation end products and mechanical stress. TGFβ, through the SMAD2 and SMAD3 cascade, plays a crucial role in this process, by accumulating ECM components. Although the three TGFβ splice forms are present in the fibrotic tissue, TGFβ1 is the key molecule responsible for the development of fibrotic tissue mainly through the activation of ALK5/SMAD2–3 signaling. Several stimuli can ativate TGFβ1, hence, increasing fibrosis, for instance, the MMPs and CTGF. MMPs stimulate TGFβ by cleaving the latent form and releasing it, whereas CTGF can bind directly to TGFβ, which stimulates the binding to the receptor and consequently its activity. However, we did not observe a significant increase in TGFβ expression, neither in these SMAD members in isolated ECs of heart and kidney, nor in the CTGF quantification. Noteworthy, like *Tgfβ2*, the *Ctgf* gene expression was slightly reduced in kidney and increased in diabetic heart in the angiogenic microarray. These findings indicate that TGFβ2 in ECs is

not involved in fibrosis in diabetic organs, a process likely attributed to fibroblasts or smooth muscle cells.

Conclusion

Altogether our findings show for the first time that the gene expression pattern implicated in energy metabolism in ECs isolated from T1DM kidneys and hearts is distinct, and accompanies different profiles of angiogenic gene expression. These findings suggest a link between metabolism and angiogenesis, and pave the way for the development of organ-specific innovative therapeutic approaches.

Acknowledgements

Funding: This work was supported by CAPES (Sciences without Border - Full Doctorate Fellowship – Process 10010-13-0); FEDER funds by COMPETE: [POCI-01-0145-FEDER-007440, POCI-01-0145-FEDER-016385]; NORTE2020 [NORTE-01-0145-FEDER-000012]; HealthyAging2020 [CENTRO-01-0145-FEDER-000012-N2323]; FCT - Fundação para a Ciência e a Tecnologia [UID/BIM/04293/2013, EXPL/BIM-MED/0492/2012, SFRH/BPD/88745/2012, SFRH/BD/111799/2015]; Claude Pepper Older Americans Independence Center; grant: P30 AG028718, NIGMS Award P20GM109096; European Structural and Investment Funds (ESIF).

Abbreviations

ADRA1A	Adrenoceptor alpha 1A
ADRA2C	Adrenoceptor alpha 2C
ALK	Activin receptor-like kinase
AMPK	AMP-activated protein kinase
CABP39	Calcium binding protein 39
CPT1A	CarnitinePalmitoyl transferase 1 A
CTGF	Connective tissue growth factor
CTR	Control
DII	Delta-like protein
DM	Diabetes mellitus
dNTPs	Deoxynucleotide triphosphates
ELISA	Enzyme-linked immunosorbent assay
ECs	Endothelial cells
FACS	Flourescence-activated cell sorting
GEP	Gene expression profile
GUSB	Beta-glucoranidase
HBSS	Hank’s balanced salt solution

KDR	Kinase insert domin receptor
MMPs	Metalloproteinases
MVD	Microvessel density
NICD	Intracellular NOTCH domain
PFKFGB2	6-phosphofructo-2-kinase/frutctose-2, 6.biphosphatase
PNPLA2	Patatin like phospholipase domain containing 2
PRKAA1	Protein kinase AMP-activated atalytic subunit alpha 1
PRKACB	cAMP-dependent protein kinase catalytic subunit beta
RB1CC1	RB1-inducible coiled-coil protein 1
RPS6KB2	Ribosomal protein S6 kinase B2
STRADA	STE20-related kinase adaptor-alpha
STZ	Streptozotocin
TGF	Transforming growth factor
TIMP	Tissue inhibitor of metalloproteinases
T1DM	Type 1 diabetes mellitus
VEGFR2	Vascular endothelial growth factor receptor-2

References

1. Associaton AD: Diagnosis and Classification of Diabetes Mellitus. Diabetes Care 2005;28:S37–42. [PubMed: 15618111]
2. Moreira JD, Pernomian L, Gomes MS, Pernomian L, Moreira RP, do Prado AF, da Silva CH, de Oliveira AM: Acute restraint stress increases carotid reactivity in type-I diabetic rats by enhancing Nox4/NADPH oxidase functionality. Eur J Pharmacol 2015;765:503–516. [PubMed: 26387612]
3. Daneman D: Type 1 diabetes. Lancet 2006;367:847–858. [PubMed: 16530579]
4. Bjornstad P, Maahs DM, Duca LM, Pyle L, Rewers M, Johnson RJ, Snell-Bergeon JK: Estimated insulin sensitivity predicts incident micro- and macrovascular complications in adults with type 1 diabetes over 6 years: the coronary artery calcification in type 1 diabetes study. J Diabetes Complications 2016;30:586–590. [PubMed: 26936306]
5. Costa PZ, Soares R: Neovascularization in diabetes and its complications. Unraveling the angiogenic paradox. Life Sci 2013;92:1037–1045. [PubMed: 23603139]
6. Cheng R, Ma JX: Angiogenesis in diabetes and obesity. Rev Endocr Metab Disord 2015;16:67–75. [PubMed: 25663658]
7. Roca F, Grossin N, Chassagne P, Puisieux F, Boulanger E: Glycation: the angiogenic paradox in aging and age-related disorders and diseases. Ageing Res Rev 2014;15:146–160. [PubMed: 24742501]
8. Dworacka M, Iskakova S, Krzyzagorska E, Wesolowska A, Kurmambayev Y, Dworacki G: Alpha-lipoic acid modifies circulating angiogenic factors in patients with type 2 diabetes mellitus. Diabetes Res Clin Pract 2015;107:273–279. [PubMed: 25511715]

9. Li FY, Lam KS, Tse HF, Chen C, Wang Y, Vanhoutte PM, Xu A: Endothelium-selective activation of AMP-activated protein kinase prevents diabetes mellitus-induced impairment in vascular function and reendothelialization via induction of heme oxygenase-1 in mice. Circulation 2012;126:1267–1277. [PubMed: 22851545]
10. Kröller-Schön S, Daiber A, Schulz E: Modulation of Vascular Function by AMPK: Assessment of NO Bioavailability and Surrogates of Oxidative Stress. Methods Mol Biol 2018;1732:495–506. [PubMed: 29480495]
11. Almabrouk TAM, White AD, Ugusman AB, Skiba DS, Katwan OJ, Alganga H, Guzik TJ, Touyz RM, Salt IP, Kennedy S: High Fat Diet Attenuates the Anticontractile Activity of Aortic PVAT via a Mechanism Involving AMPK and Reduced Adiponectin Secretion. Front Physiol 2018;9:51. [PubMed: 29479319]
12. Schindelin J, Arganda-Carreras I, Frise E, Kaynig V, Longair M, Peitzsch T, Preibisch S, Rueden C, Saalfeld S, Schmid B, Tinevez JY, White DJ, hartenstein V, Eliceiri K, Tomancak P, Cardona A: Fiji: an open-source platform for biological-image analysis. Nat Methods 2012;9:676–682. [PubMed: 22743772]
13. Waltenberger J: VEGF resistance as a molecular basis to explain the angiogenesis paradox in diabetes mellitus. Biochem Soc Trans 2009;37:1167–1170. [PubMed: 19909240]
14. Tchaikovski V, Olieslagers S, Bohmer FD, Waltenberger J: Diabetes mellitus activates signal transduction pathways resulting in vascular endothelial growth factor resistance of human monocytes. Circulation 2009;120:150–159. [PubMed: 19564559]
15. Costa R, Rodrigues I, Guardao L, Lima JQ, Sousa E, Soares R, Negrao R: Modulation of VEGF signaling in a mouse model of diabetes by xanthohumol and 8-prenylnaringenin: Unveiling the angiogenic paradox and metabolism interplay. Mol Nutr Food Res 2017; DOI:10.1002/mnfr.201600488.
16. Cunha SI, Pietras K: ALK1 as an emerging target for antiangiogenic therapy of cancer. Blood 2011;117:6999–7006. [PubMed: 21467543]
17. David L, Mallet C, Mazerbourg S, Feige J-J, Bailly S: Identification of BMP9 and BMP10 as functional activators of the orphan activin receptor-like kinase 1 (ALK1) in endothelial cells. Blood 2007;109:1953–1961. [PubMed: 17068149]
18. Scharpfenecker M, van Dinther M, Liu Z, van Bezooijen RL, Zhao Q, Pukac L, Löwik CWGM, ten Dijke P: BMP-9 signals via ALK1 and inhibits bFGF-induced endothelial cell proliferation and VEGF-stimulated angiogenesis. J Cell Sci 2007;120:964–972. [PubMed: 17311849]
19. Pagie S, Gerard N, Charreau B: Notch signaling triggered via the ligand DLL4 impedes M2 macrophage differentiation and promotes their apoptosis. Cell Commun Signal 2018;16:4. [PubMed: 29321062]
20. Kopan R, Ilagan MXG: The Canonical Notch Signaling Pathway: Unfolding the Activation Mechanism. Cell 2009;137:216–233. [PubMed: 19379690]
21. Nandagopal N, Santat LA, LeBon L, Sprinzak D, Bronner ME, Elowitz MB: Dynamic Ligand Discrimination in the Notch Signaling Pathway. Cell 2018;172:869–880.e19. [PubMed: 29398116]
22. Soares R, Balogh G, Guo S, Gartner F, Russo J, Schmitt F: Evidence for the notch signaling pathway on the role of estrogen in angiogenesis. Mol Endocrinol 2004;18:2333–2343. [PubMed: 15192074]
23. Benedito R, Roca C, Sörensen I, Adams S, Gossler A, Fruttiger M, Adams RH: The Notch Ligands Dll4 and Jagged1 Have Opposing Effects on Angiogenesis. Cell 2009;137:1124–1135. [PubMed: 19524514]
24. Pedrosa AR, Trindade A, Fernandes AC, Carvalho C, Gigante J, Tavares AT, Diéguez-Hurtado R, Yagita H, Adams RH, Duarte A: Endothelial Jagged1 Antagonizes Dll4 Regulation of Endothelial Branching and Promotes Vascular Maturation Downstream of Dll4/Notch1. Arteriosclerosis, Thrombosis, and Vascular Biology 2015;35:1134–1146.
25. Pedrosa AR, Trindade A, Carvalho C, Graça J, Carvalho S, Peleteiro MC, Adams RH, Duarte A: Endothelial Jagged1 promotes solid tumor growth through both pro-angiogenic and angiocrine functions. Oncotarget 2015;6:24404–24423. [PubMed: 26213336]
26. Guo X, Wang XF: Signaling cross-talk between TGF-beta/BMP and other pathways. Cell Res 2009;19:71–88. [PubMed: 19002158]

27. Brew K, Nagase H: The tissue inhibitors of metalloproteinases (TIMPs): An ancient family with structural and functional diversity. Biochim Biophys Acta 2010;1803:55–71. [PubMed: 20080133]
28. Ruiz-Ortega M, Rodriguez-Vita J, Sanchez-Lopez E, Carvajal G, Egido J: TGF-beta signaling in vascular fibrosis. Cardiovasc Res 2007;74:196–206. [PubMed: 17376414]
29. Schiller M, Javelaud D, Mauviel A: TGF-beta-induced SMAD signaling and gene regulation: consequences for extracellular matrix remodeling and wound healing. J Dermatol Sci 2004;35:83–92. [PubMed: 15265520]
30. Yang L, Pang Y, Moses HL: TGF-beta and immune cells: an important regulatory axis in the tumor microenvironment and progression. Trends Immunol 2010;31:220–227. [PubMed: 20538542]
31. Berk BC: Vascular Smooth Muscle Growth: Autocrine Growth Mechanisms. Physiol Rev 2001;81:999–1030. [PubMed: 11427690]
32. Cooper ME, Vranes D, Youssef S, Stacker SA, Cox AJ, Rizkalla B, Casley DJ, Bach LA, Kelly DJ, Gilbert RE: Increased renal expression of vascular endothelial growth factor (VEGF) and its receptor VEGFR-2 in experimental diabetes. Diabetes 1999;48:2229–2239. [PubMed: 10535459]
33. Okar DA, Lange AJ, Manzano À, Navarro-Sabatè A, Riera Ls, Bartrons R: PFK-2/FBPase-2: maker and breaker of the essential biofactor fructose-2,6-bisphosphate. Trends Biochem Sci 2001;26:30–35. [PubMed: 11165514]
34. Manzano A, Rosa JL, Ventura F, Pérez JX, Nadal M, Estivill X, Ambrosio S, Gil J, Bartrons R: Molecular cloning, expression, and chromosomal localization of a ubiquitously expressed human 6-phosphofructo-2-kinase: fructose-2, 6-bisphosphatase gene (PFKFB3). Cytogenet Cell Genet 1998;83:214–217. [PubMed: 10072580]
35. De Bock K, Georgiadou M, Schoors S, Kuchnio A, Wong BW, Cantelmo AR, Quaegebeur A, Ghesquiere B, Cauwenberghs S, Eelen G, Phng LK, Betz I, Tembuyser B, Brepoels K, Welti J, Geudens I, Segura I, Cruys B, Bifari F, Decimo I, et al.: Role of PFKFB3-driven glycolysis in vessel sprouting. Cell 2013;154:651–663. [PubMed: 23911327]
36. Eelen G, de Zeeuw P, Simons M, Carmeliet P: Endothelial cell metabolism in normal and diseased vasculature. Circ Res 2015;116:1231–1244. [PubMed: 25814684]
37. Draoui N, de Zeeuw P, Carmeliet P: Angiogenesis revisited from a metabolic perspective: role and therapeutic implications of endothelial cell metabolism. Open Biol 2017;7:pii:170219. [PubMed: 29263247]
38. Fisslthaler B, Fleming I: Activation and signaling by the AMP-activated protein kinase in endothelial cells. Circ Res 2009;105:114–127. [PubMed: 19608989]
39. Mihaylova MM, Shaw RJ: The AMPK signalling pathway coordinates cell growth, autophagy and metabolism. Nat Cell Biol 2011;13:1016–1023. [PubMed: 21892142]

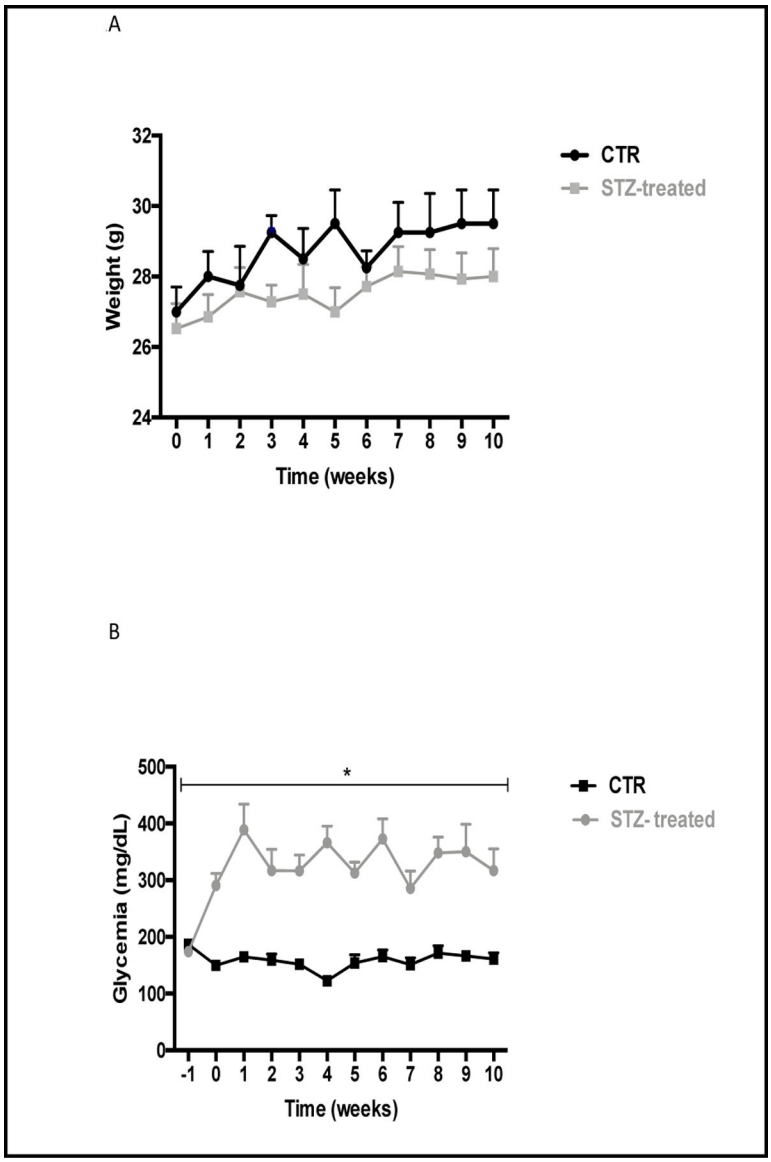

Fig. 1.

Body weight (A) and glycemia (B) in T1DM (STZ-treated) and healthy (CTR) mice for 10 weeks after STZ administration. Week −1 in glycemia graph refers to glycemia one week before STZ administration. (*p< 0.05 STZ vs Control).

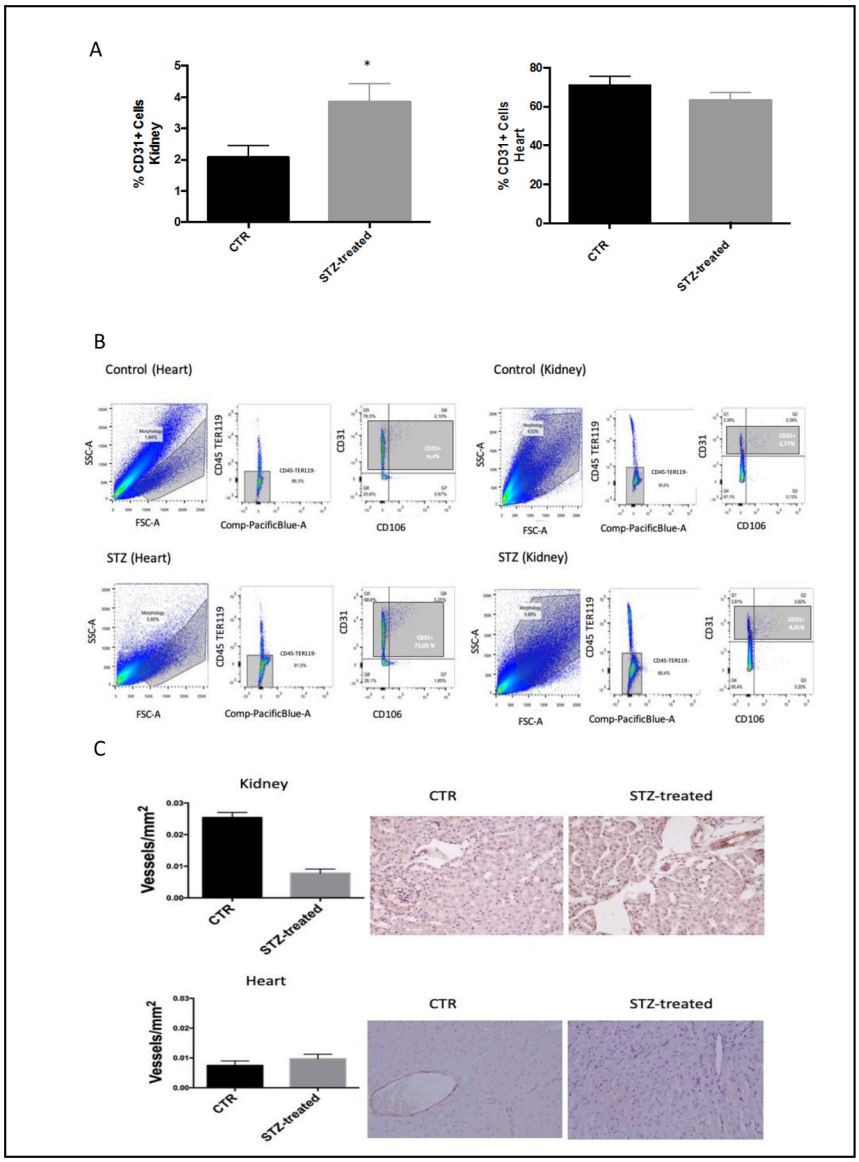

Fig. 2.

(A) Number of CD31-positive cells in kidney and heart assessed by FACS-based ECs isolation from of control and T1DM animals. Values are in percentage of total number of cells. (B) Representative plots showing the discrimination of endothelial cells (CD31+) isolated from the left ventricle and kidneys of control and STZ-induced diabetic mice after exclusion of hematopoietic (CD45+) and erytroid (TER119+) cells. (C) Microvessel density in kidney and heart of STZ-treated and control animals by immunohistocheminstry against CD31. Values correspond to the number of vessels per total tissue area. p value ≤ 0.05. Images magnification x200.

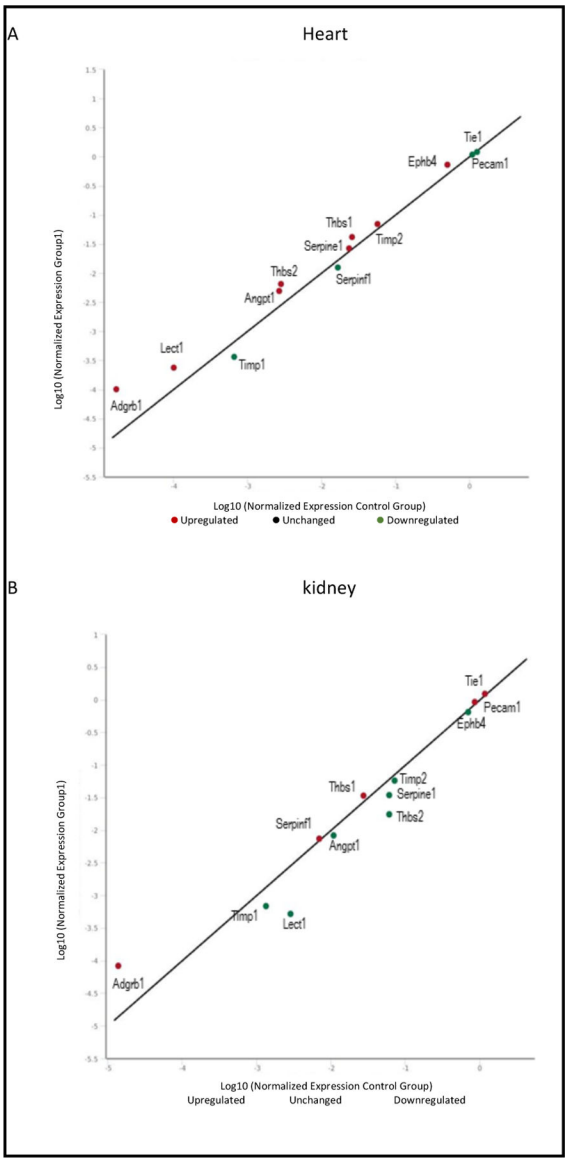

Fig. 3.

The antiangiogenic gene expression profile analysis in heart (A) and kidney (B) of control and T1DM animals. Values represent fold change of STZ-treated vs control animals. Red spots are upregulated genes; Green spots are downregulated genes.

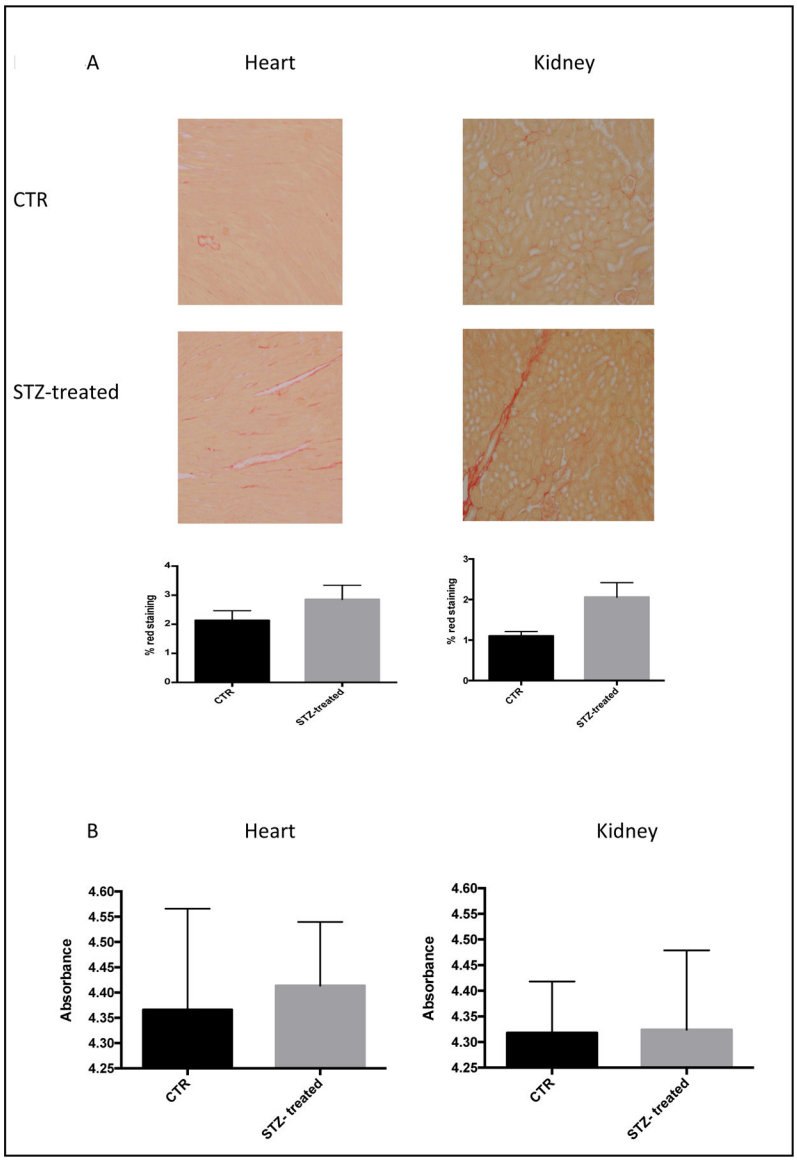

Fig. 4.

Fibrosis analyses in heart and kidney of control and T1DM animals. (A) Sirius red histological staining of STZ-treated and control mice. Graphs illustrate the quantification of red stained area, shown in histological images. Magnification X200. (B) CTGF quantification by ELISA assay in both organs of STZ-treated and control mice.

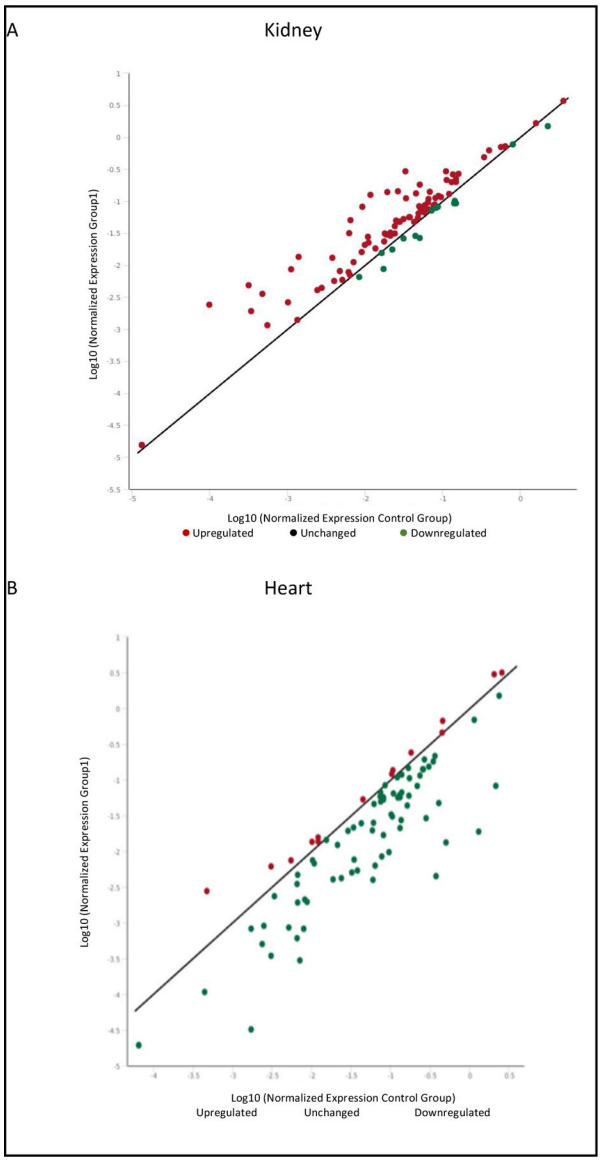

Fig. 5.

AMPK signaling gene expression profile analysis in kidney (A) and heart (B) of control and T1DM animals. Values represent fold change of STZ-treated vs control animals. Red spots are upregulated genes; Green spots are down regulated genes.

Table 1.

Primer sequences used for real-time PCR assay

Genes	Sequence
ADRA1A	Forward: GATGACACTAGGGCTTTTATC
	Reverse: GTCAAGTTCACTCCTTCATC
ADRA2C	Forward: AAGTTTTTCTTCTGGATCGG
	Reverse: GAGGATATGCTTGAAAGAGC
CPT1-A	Forward: GGGAGGAATACATCTACCTG
	Reverse: GAAGACGAATAGGTTTGAGTTC
GAPDH	Forward: AGCCTCGTCCCGTAGACAAAA
	Reverse: GATGACAAGCTTCCCATT
JAG1	Forward: GCAAGACTTGTCAGTTAGATG
	Reverse: CTGGCAATCAGATTCTTACAG
PFKFB2	Forward: GAGGCTAGAACAGGAAGTTA
	Reverse: CACATTAGGCAGATCTCCAG
PNPLA2	Forward: CTTAGGAGGAATGCCCTG
	Reverse: TTCATCCACCGGATATCTTC
SMAD5	Forward: TTTGCAGAGCCATCACGAGC
	Reverse: TTTCCAATATGCCGCCTAGT
TGFB2	Forward: ATGCCCATATCTATGGAGTTC
	Reverse: TAGAGAATGGTCAGTGGTTC
TIMP2	Forward: GGATTCAGTATGAGATCAAGC
	Reverse: GCCTTTCCTGCAATTAGATAC

Table 2.

Angiogenic gene expression significantly altered in ECs of heart of diabetic animals.

Genes	Fold Change *	P-Value
Jag1	0.82	0.033
Smad5	1.37	0.022

* Values indicated are fold change relative to healthy controls. Values in red are the upregulated genes and in green are the downregulated genes (p value < 0.05)

Table 3.

Angiogenic gene expression significantly altered in ECs of kidney of diabetic animals.

Genes	Fold Change *	P-Value
Kdr	0.75	0.041
Tgfβ2	0,70	0.046
Timp2	0.80	0.048

* Values indicated are fold change relative to healthy controls. Values in green are the downregulated genes (p value < 0.05)

Table 4.

AMPK-dependent gene expression significantly altered in ECs from heart of diabetic animals.

Genes	Fold Change *	P-Value
Cab39 Calcium binding proitein 39	0.539	0.043
Akt2 Serine/threonine kinase 2	0.380	0.041
Adra2c Adrenoceptor α2c	0.286	0.011
Pnpla2 Patatin-like phospholipase domain containing 2	0.715	0.010
Prkacb cAMP-dependent protein kinase catalytic subunit β	0.520	0.007
Rps6kb2 Ribosomal protein S6 kinase B2	0.323	0.022

*Values indicated are fold change relative to healthy controls. Values in green are the downregulated genes (p value < 0.05)

Table 5.

AMPK-dependent Gene expression significantly altered in ECs from kidney of diabetic animals.

Genes	Fold Change *	P-Value
Adra1a Adrenoceptor α1a	3.47	0.032
Cpt1a Carnitine pamitoyl transferase 1A	1.92	0.007
Gusb β-Glucoronidase	1.63	0.020
Prkaa1 Protein kinase AMP-Activated catalytic subunit Alpha 1	1.49	0.012
Pfkfb2 6-phosphofructo-2-kinase/fructose-2,6-bisphosphatase	1.79	0.042
Strada STE20-related adapter-alpha	1.52	0.013
Rb1cc1 Rb1 inducible coiled-coil protein 1	1.32	0.022

* Values indicated are fold change relative to healthy controls. Values in red are the upregulated genes (p value < 0.05)